



Modeling miniband for realistic silicon nanocrystal array

Weiguo Hu^{a,b}, Mohd Fairuz Budiman^{a,b}, Makoto Igarashi^{a,b}, Ming-Yi Lee^c, Yiming Li^{c,d},
Seiji Samukawa^{a,b,d,*}

^a Institute of Fluid Science, Tohoku University, 2-1-1 Katahira, Aoba-ku, Sendai, Miyagi 980-8577, Japan

^b Japan Science and Technology Agency (JST), CREST, 5 Sanbancho, Chiyoda, Tokyo 102-0075, Japan

^c Parallel and Scientific Computing Laboratory, Department of Electrical and Computer Engineering, National Chiao Tung University, Hsinchu 300, Taiwan

^d WPI Advanced Institute for Materials Research, Tohoku University, 2-1-1 Katahira, Aoba, Sendai, 9808577, Japan

ARTICLE INFO

Keywords:

Finite element method
Miniband
Quantum dot solar cell

ABSTRACT

Within the envelop-function framework, we developed the finite element method to calculate the minibands in the realistic Silicon nanocrystal array. This method clearly reveals the miniband formation and accurately calculates the E - K dispersion relationship. In the simple 1D array, the deduced miniband structure matches well with the analytic Kronig–Penney method. More importantly, it can better simulate the 2D and 3D nanocrystal array, which avoids approximations of the quantum cubic box and the independent periodic potential of the multi-dimension Kronig–Penney method. Further, this model is utilized to calculate miniband structure of realistic 2D-array Silicon nanodisk array for guiding quantum dot solar cell design.

© 2012 Elsevier Ltd. All rights reserved.

1. Introduction

The quantum dots (QDs) solar cell is a promising candidate for the next-generation ultra-high efficiency solar cell. For example, with working as the intermediate band solar cell, its theoretical conversion efficiency exceeds 63%, which aroused great interest in the theoretical and experimental researches [1–6]. When uniform QDs are closely packed as the superlattice, the wavefunction diffuses into neighboring QDs and couples with each other to broaden the discrete quantum levels to form finite-width minibands. Minibands structure is the key parameters for QDs solar cell application, which determines two-photon transition and photo-generation carrier transport. With approximations of the quantum cubic box and the independent periodic potential, the analytic Kronig–Penney method is developed to describe the high-dimension QDs superlattices, which offer much significant information for QDs solar cell design [7,8]. With the great development of nanotechnologies and device processes, the more accurate method should be developed to instruct realistic QDs fabrication. For example, well-developed Stranski–Krastanow technology commonly fabricates sphere, lens or even irregular QD with mixture 2D quantum state of wetting layer. Especially, a promising top-down nanotechnology, neutral beam etching combined with bio-template, provides greater flexibility in engineering quantum structures such as independently adjustable diameter, thickness, interdot space, incline angle, matrix materials and so on [9,10]. The finite element method (FEM) is an intuitive and effective technology to simulate the complex and realistic physics properties, such as strain distribution, surface potential and energy band structure [11,12].

* Corresponding author at: Institute of Fluid Science, Tohoku University, 2-1-1 Katahira, Aoba-ku, Sendai, Miyagi 980-8577, Japan. Tel.: +81 22 217 5240; fax: +81 22 217 5240.

E-mail address: samukawa@ifs.tohoku.ac.jp (S. Samukawa).

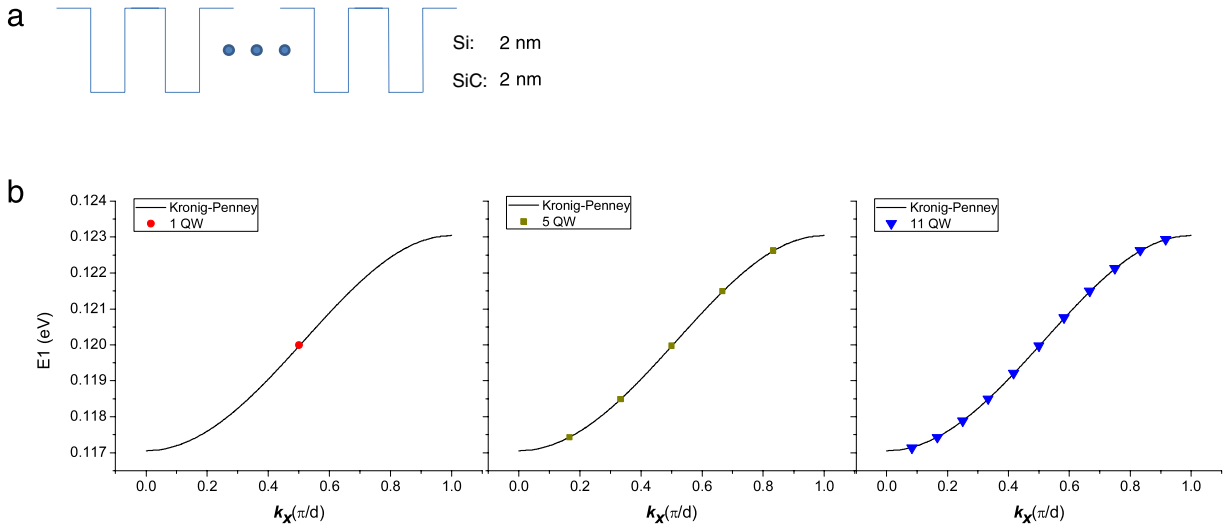


Fig. 1. (a) Structure sketch of 1D Si/SiC superlattice. (b) The E - K dispersions calculated by the Kronig–Penney model (Solid line), and FEM (dot plots) with 1, 5, 11 wells.

In this paper, we develop the finite element method to simulate minibands structure in a realistic and arbitrary QD array. This method settles down well theoretical approximations of the high-dimensional Kronig–Penney method and reveals some significant information for 2D array Silicon nanodisc design.

2. The computational model

With the one-band envelop-function theory, the electronic structure is described as the Schrödinger equation:

$$-\nabla \cdot \left(\frac{\hbar^2}{2m} \nabla \varphi \right) + V\varphi = E\varphi \tag{1}$$

where \hbar , m , V , E , φ are Planck’s constant divided by 2π , the effective mass, the position-dependent potential energy, quantum levels, and the electron envelope function, respectively. The Si-based solar cell has very significant commercial value. Here, we suggest developing an Si/3C–SiC quantum dot for solar cell application, and their physics constants are used as input parameters. The complex quantum structure is discretized in the real space with the FEM [13]. The nonuniform mesh is adopted to greatly speed up the calculation process. The discretized Schrodinger equation forms a serial of partial differential equations, and is solved as the eigenvalue problem. The FEM is a variation reformulation and keeps the wavefunction continuous at interfaces. To approach the infinite superlattice, the Dirac-boundary is set at least 10 times larger than the QD array total length.

Firstly, we consider a simply 1 dimensional Si/SiC quantum well, as shown in the Fig. 1(a). In the single well, the wavefunction is localized and forms a serials of discrete levels; with increasing the well numbers, their wavefunctions are coupled with each other and result in the level splitting, and finally form broaden minibands. Here, the number of states in every miniband is equal to the number of wells.

In an infinite superlattice, the wavefunction has the Bloch wave form:

$$\varphi_{nk}(r) = e^{ik \cdot r} \phi_{nk}(r). \tag{2}$$

Thus, if the superlattice grain is enough large, the sublevel order has the below relationship with the Bloch vector, k , [13,14]

$$k = \frac{i\pi}{(N+1)d}, \quad i = 1 : N, \tag{3}$$

where, N is the well number and d is the periodic length of grain. With this relationship, we can develop the FEM to calculate the E - K dispersion relationship. The multi-dimension case can be treated as a multi orthometric wave vector.

With the Bloch theorem, the simple 1D superlattice can get an analytical solution, the classic Kronig–Penney method [7],

$$\cos(kd) = \cos(\alpha a) \cosh(\beta b) - \frac{1}{2} \left(\frac{\alpha}{\beta} \frac{m_b}{m_w} - \frac{\beta}{\alpha} \frac{m_w}{m_b} \right) \sin(\alpha a) \sinh(\beta b), \tag{4}$$

where d is the sum of the well thickness and the barrier thickness, m_i is the effective mass in the well or barrier. This analytic resolution is used to verify our developed FEM. However, for multiple dimensions, the Kronig–Penney method needs extra approximations, for example, the quantum cubic box and the independent periodic potential.

	V		V	
V	2V	V	2V	V
	V		V	
V	2V	V	2V	V
	V		V	

Fig. 2. Independent periodic potential approximation for multi-dimension Kronig–Penney method $V(r) = V(x) + V(y)$.

3. Numerical results and discussion

Fig. 1 reveals a 1D Si/SiC superlattice. The structure sketch is shown as the Fig. 1(a). In the 1D case, the Kronig–Penney model can accurately calculate the E – K dispersion relationship without extra approximation, shown as the solid line in Fig. 1(b). Results of our FEM are shown as the solid circle, square and triangle responding to 1, 5, 11 wells, respectively. From this figure, we can find that the sub-levels correspond well with the energy in the same wave vector; and with increasing the well number, dot plots gradually approach the ideal E – K dispersion. According to Eq. (4), the E – K dispersion follows exponential relationship, thus has very small difference at the two bottoms. Thus, we think that more than 11 wells per array is enough to describe the whole miniband.

In more dimensions, the relationship between sub level order and Bloch vector can be simply treated as a multi-orthometric 1D relationship. However, the multidimensional Kronig–Penney method has to take the below approximation,

$$V(r) = V(x) + V(y). \quad (5)$$

Then, E – K dispersion can be treated as the vector sum of the independent 1D case. A major problem lies in that the above potential overestimates the potential at the diagonal corner, $2V$ at the shade zone ($3V$ for 3D case), as shown in Fig. 2. Obviously, this method only deals with the rectangle or cubic dot.

2D rectangle structure and the first-Brillouin zone (FBZ) are shown Fig. 3(a), and the E – K dispersion calculated by the FEM (solid circle) and Kronig–Penney method (solid line) are shown in the Fig. 3(b). Whole trends of this two method are very similar; due to effects of periodic potential, the ground level gradually increases along Γ – X – M crystal direction, and returned to Γ point, which forms 2D in-plan minibands. For a more accurate comparison, we found that in this 2D case, the Kronig–Penney method underestimates the E – K dispersion, especially along the Γ – M direction, the diagonal direction, and the difference is near to 5 meV around the M point. It is reasonable in physics; the overestimated potential in diagonal zone decreases the wavefunction diffusion probability into the neighbor dots to weaken the energy dispersion.

Due to low potential surface potential, the realistic quantum dot inclines to form a circle or spherical interface. In Fig. 4, we compare the rectangle quantum dot and circle quantum dot array. We found that the circle dot markedly increases the minibands' energy, more than 24 meV around the M point. A major reason is that the circle quantum dot decreases the average quantum confinement size to increase the confinement energy. If we up-shift the rectangle dot minibands with confinement energy difference in single dot, the E – K dispersion of the square dot is weakly stronger than that of the circle dot, which can be attributed to the increased average inter-dot space. Thus, for some rough estimation with the Kronig–Penney method, a considerable amendment is to add an additional confinement energy difference in the rectangle or cubic dot.

A top-to-down nanotechnology, neutral beam etching combined with a bio-template, becomes promising for an ultra-high quality QD array with high uniformity, quasi-crystal alignment, and high sheet density [9,10]. The FEM is used to calculate the miniband structures of this realistic 3D nanodisk. Due to the balance of interactions such as chemical bonding, Coulomb potential and so on, the hexagonal alignment, for example Wurtzite structure, is a common crystal structure. We build up the below model to describe a realistic Si/SiC 2D array. A structure sketch is shown in Fig. 5(a). FEM is used to discretize the Schrodinger equation in the real space. The nonuniform mesh is adopted to greatly speed up the calculation process, as shown in Fig. 5(b). The minimum mesh is 0.02 nm, which is far smaller than single QD size and used to describe the internal interfaces. In one case, the total mesh is around 1.2 million and costs 16 GB of memory. A common workstation can resolve these partial differential equations well. The FEM model also can be used to calculate a more complex, realistic and large structure, for example cubic or Wurtzite-like QD superlattice. In that case, optimizing arithmetic to deduce the mesh total or parallel program in clusters can effectively speed up the calculation.

As shown in Fig. 5(c), we want to point out that ND fabricated by the top-to-down process is a special quantum dot structure with two independently controllable structure parameters, diameter and thickness, which breaks the symmetric of atomic orbit so that the 3-fold degenerate p -orbit becomes a 2-fold degenerate (121) orbit and nondegenerate (210) orbit. In cylindrical coordinates, the wavefunction is therefore expressed as

$$\Psi = \cos(lz)J_m(mr) \exp(in\theta), \quad l = 1, \dots, \infty, \quad m = 1, \dots, \infty, \quad |n| = 0, \dots, m - 1, \quad (6)$$

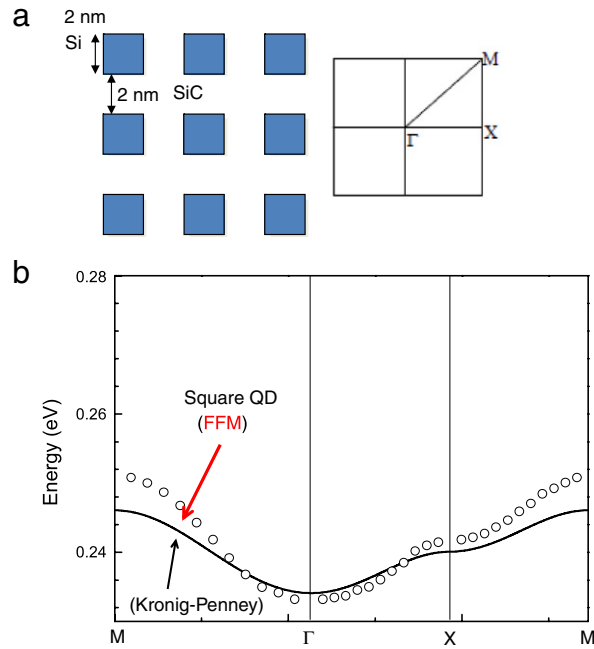


Fig. 3. (a) The square QD 2D array and the first Brillouin zone. (b) The E - K dispersions calculated by the Kronig-Penney model (Solid line), and FEM (dot plots).

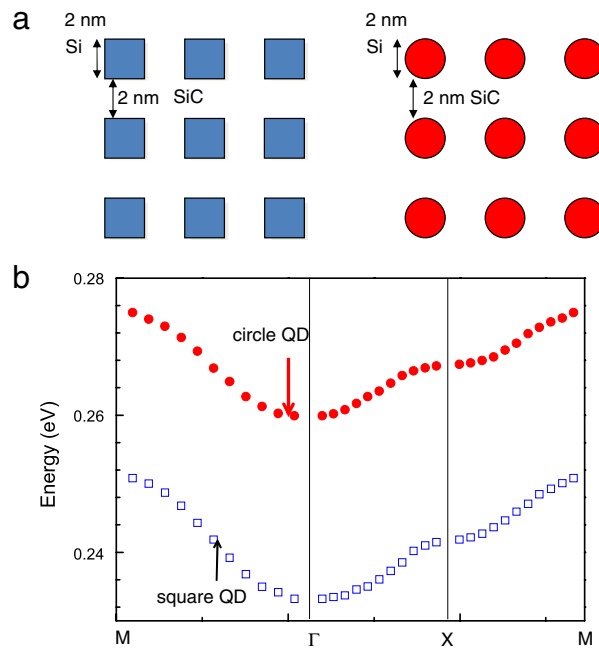


Fig. 4. (a) The square QD 2D array and the circle QD 2D array. (b) The E - K dispersions.

where, l, m, n are three main quantum numbers, which denote different minibands. These two independently controllable structure parameters bring higher flexibility in miniband design, for example the more controllable bandgap and sub-bandgap.

Minibands' level and width are the key parameters for solar cell application. Fig. 6 reveals a minibands structure in a serial of QD array with different diameter and thickness. The important regulation is that miniband positions inverse-squarely decrease with increasing thickness and diameter, which is determined by the classic quantum size effect; due to in-plane wavefunction coupling, the minibands' width strongly depends on the diameter and is basically independent of the

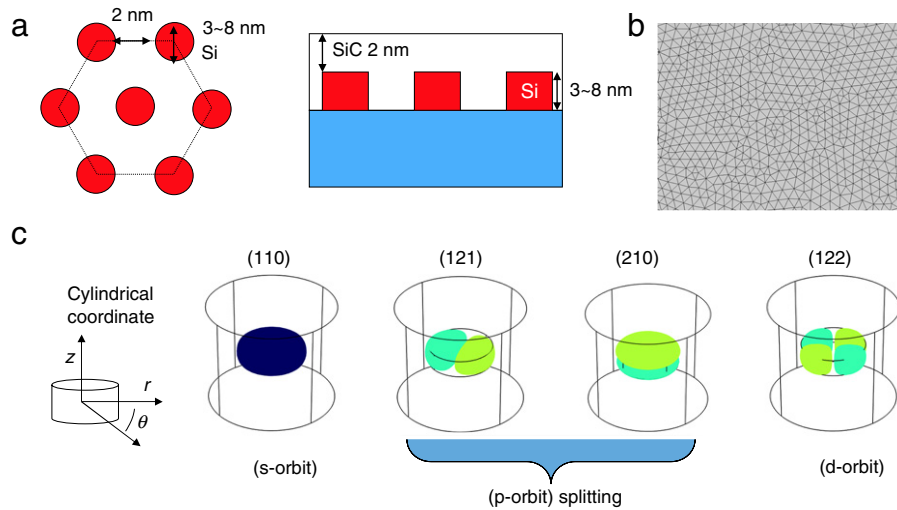


Fig. 5. (a) Realistic Si/SiC ND 2D array. (b) Nonuniform mesh for calculation. (c) Electron wavefunction and quantum numbers.

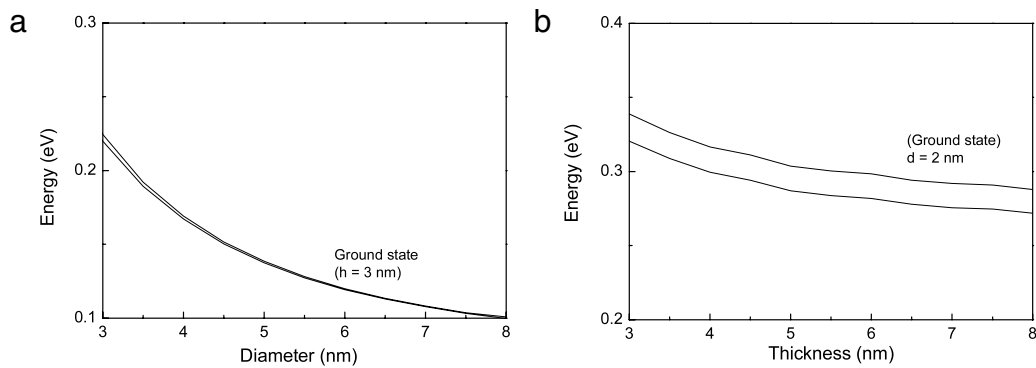


Fig. 6. The minibands structure depends on (a) the thickness, and (b) diameter.

thickness. In addition, those minibands' absolute values are also helpful for verifying our experimental results and further guide QD solar cell design [15].

4. Conclusions

The FEM is developed to calculate the minibands structure in a nanocrystal array. In the simple 1D array, this method matches well with the analytic Kronig–Penney method, and without extra approximation, it can be simply developed to a 2D or 3D realistic nanocrystal array. By comparing to multi-dimensional Kronig–Penney, we have an intuitionistic understanding about the effects of the quantum cubic box and the independent periodic potential in rough estimation. Further, this model is utilized to calculate miniband structure of a realistic 2D-array Silicon nanodisk array for guiding quantum dot solar cell design.

References

- [1] A. Luque, A. Martí, C. Stanley, Understanding intermediate-band solar cells, *Nat. Photon.* 6 (3) (2012) 146–152.
- [2] Y. Okada, T. Morioka, K. Yoshida, R. Oshima, Y. Shoji, T. Inoue, T. Kita, Increase in photocurrent by optical transitions via intermediate quantum states in direct-doped InAs/GaNAs strain-compensated quantum dot solar cell, *J. Appl. Phys.* 109 (2) (2011) 024301. pp. 1–5.
- [3] W. Hu, Y. Harada, A. Hasegawa, T. Inoue, O. Kojima, T. Kita, Intermediate band photovoltaics based on interband–intra-band transitions using In_{0.53}Ga_{0.47}As/InP superlattice, *Prog. Photovolt. Res. Appl.* (2011) <http://dx.doi.org/10.1002/pip.1208>.
- [4] C.C. Lin, W.L. Liu, C.Y. Shih, Detailed balance model for intermediate band solar cells with photon conservation, *Opt. Express* 19 (18) (2011) 16927–16933.
- [5] K. Yoshida, Y. Okada, N. Sano, Self-consistent simulation of intermediate band solar cells: effect of occupation rates on device characteristics, *Appl. Phys. Lett.* 97 (13) (2010) 133503. pp. 1–3.
- [6] A.S. Lin, W. Wang, J.D. Phillips, Model for intermediate band solar cells incorporating carrier transport and recombination, *J. Appl. Phys.* 105 (6) (2009) 064512. pp. 1–8.
- [7] O.L. Lazarenkova, A.A. Balandin, Miniband formation in a quantum dot crystal, *J. Appl. Phys.* 89 (10) (2001) 5509–5515.

- [8] C.W. Jiang, M.A. Green, Silicon quantum dot superlattices: modeling of energy bands, densities of states, and mobilities for silicon tandem solar cell applications, *J. Appl. Phys.* 99 (11) (2006) 114902. pp. 1–7.
- [9] M.F. Budiman, W. Hu, M. Igarashi, R. Tsukamoto, T. Isoda, K.M. Itoh, I. Yamashita, A. Murayama, Y. Okada, S. Samukawa, Control of optical bandgap energy and optical absorption coefficient by geometric parameters in sub-10 nm silicon-nanodisc array structure, *Nanotechnology* 23 (6) (2012) 065302. pp. 1–6.
- [10] C.-H. Huang, X.-Y. Wang, M. Igarashi, A. Murayama, Y. Okada, I. Yamashita, S. Samukawa, Optical absorption characteristic of highly ordered and dense two-dimensional array of silicon nanodiscs, *Nanotechnology* 22 (10) (2011) 105301. pp. 1–8.
- [11] Yiming Li, An iterative method for single and vertically stacked semiconductor quantum dots simulation, *Math. Comput. Modelling* 42 (7–8) (2005) 711–718.
- [12] Yiming Li, Transition energies in vertically coupled multilayer nanoscale InAs/GaAs semiconductor quantum dots with different structure shapes, *Japanese J. Appl. Phys.* 44 (4B) (2005) 2642–2646.
- [13] P. Pereyra, E. Castillo, Theory of finite periodic systems: general expressions and various simple and illustrative examples, *Phys. Rev. B* 65 (20) (2002) 205120. pp. 1–26.
- [14] C. Galeriu, L.C. Lew Yan Voon, R. Melnik, M. Willatzen, Modeling a nanowire superlattice using the finite difference method in cylindrical polar coordinates, *Comput. Phys. Comm.* 157 (2) (2004) 147–159.
- [15] W.G. Hu, T. Inoue, O. Kojima, T. Kita, Effects of absorption coefficients and intermediate-band filling in InAs/GaAs quantum dot solar cells, *Appl. Phys. Lett.* 97 (19) (2010) 193106. pp. 1–3.